Water-Gas Shift Reaction Produces Formate at Extreme Pressures and Temperatures in Deep Earth Fluids

Nore Stolte,[†,‖] Junting Yu,[†,‖] Zixin Chen,[‡] Dimitri A. Sverjensky,[¶] and Ding Pan[*,†,‡,§]

†Department of Physics, Hong Kong University of Science and Technology, Hong Kong, China

‡Department of Chemistry, Hong Kong University of Science and Technology, Hong Kong, China

¶Department of Earth and Planetary Sciences, Johns Hopkins University, 3400 North Charles Street, Baltimore, MD 21218, USA

§HKUST Fok Ying Tung Research Institute, Guangzhou, China

‖These authors contributed equally to this work.

E-mail: dingpan@ust.hk

Abstract

The water-gas shift reaction is one of the most important reactions in industrial hydrogen production and plays a key role in Fischer-Tropsch-type synthesis, which is widely believed to generate hydrocarbons in the deep carbon cycle, but is little known at extreme pressure-temperature conditions found in Earth's upper mantle. Here, we performed extensive ab initio molecular dynamics simulations and free energy calculations to study the water-gas shift reaction. We found the direct formation of formic acid from CO and supercritical water at 10∼13 GPa and 1400 K without any catalyst. Contrary to the common assumption that formic acid or formate is an intermediate product, we found that HCOOH is thermodynamically more stable than the products of the water-gas shift reaction above 3 GPa and at 1000∼1400 K. Our study suggests that the water-gas shift reaction may not happen in Earth's upper mantle, and formic acid or formate may be an important carbon carrier in reducing environments, participating in many geochemical processes in deep Earth.

Graphical TOC Entry
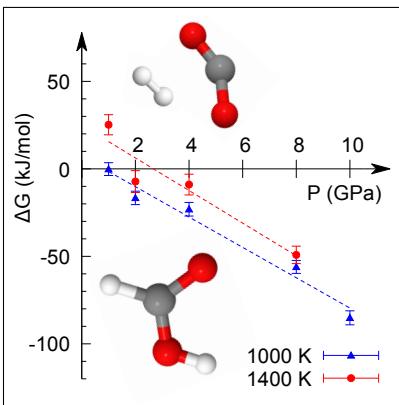
Carbon is a unique element for all known life on Earth. Its oxidation state varies from -4 to +4, which gives it very rich chemical bonding environments. More than 90% of Earth's carbon is stored in its interior,[1] and the deep carbon cycle substantially influences climate change over geologic time and human energy consumption near Earth's surface, with a critical impact on human sustainable development.[2] Although as early as the 19th century, Mendeleev proposed that petroleum might be formed by abiogenic means,[3] only over the past few decades have scientists started to seriously evaluate the possibility of hydrocarbon generation from subducting carbon and water in the deep carbon cycle.[4,5] Hydrocarbons may play a key role in the formation of diamonds,[6-9] the possible origin of abiogenic petroleum[5] and even deep life;[10] however, the formation of hydrocarbons is little known at extreme conditions found in Earth's upper mantle, where pressure (P) may reach ~13 GPa and temperature (T) as high as 1700 K.[11,12]

Fischer-Tropsch-type synthesis, which in general refers to converting inorganic carbon to organic matter, has been widely believed to naturally happen in deep Earth environments,[4,5] but most of our knowledge is limited to industrial applications, where P-T conditions are not as severe as in Earth's interior and purpose-designed catalysts are crucial.[13] In Fischer-Tropsch-type processes, the water-gas shift reaction is a key reaction to balance the CO/H_2 ratio:[14]

$$CO(g) + H_2O(g) \rightleftharpoons CO_2(g) + H_2(g). \tag{1}$$
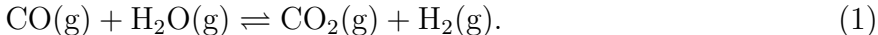
This reaction is exothermic (-41 kJ/mol at 0.1 MPa and 298 K), but has a large reaction barrier, so industry usually uses transition metal catalysts, e.g, Fe-Cr and Cu-Zn, at above-ambient conditions: 1-6 MPa and 450-720 K.[15] The reaction mechanism varies with different catalysts, but industrial catalysts usually do not exist in deep Earth.[4] Some studies suggest that formic acid (HCOOH) or formate ($HCOO^-$) may be a possible reaction intermediate in the catalyzed[16] and uncatalyzed[17] reactions. Sharma et al. started experiments from formic acid to study C-H-O fluids in a reducing environment, and found that HCOOH fully decomposes into CO_2, H_2, CO, and H_2O when P is lower than 0.5 GPa and T is above 623

K.[18]

C-H-O fluids in the deep crust and upper mantle are a fundamentally important carbon carrier in the deep carbon cycle, and were traditionally modeled as simple mixtures of small volatile molecules, e.g. H_2O, CO_2, CO, CH_4, H_2.[19] Recently, experimental and theoretical studies have started to consider aqueous ions, complexes, and chemical speciation in C-H-O fluids,[8,20–25] and many of them focus on fully oxidized carbon forms in supercritical water.[26–29] With increasing depth, Earth's interior becomes more reducing,[30] so reduced carbon is of great importance in deep Earth, but due to the lack of reliable data at extreme P-T conditions, the water-gas shift reaction was simply assumed to adjust the fluid composition in reducing environments.[18,31]

Here, by performing extensive ab initio molecular dynamics (AIMD) simulations, we studied mixtures of CO and H_2O and reaction products at extreme P-T conditions found in Earth's upper mantle. Without any empirical input, AIMD simulations have grown to be powerful tools to predict chemical speciation at extreme conditions from first principles,[32–34] and many predictions were confirmed by later experiments (e.g., refs 21,26–28). We found that CO directly reacts with H_2O to generate formic acid at 10∼13 GPa and 1400 K without any catalyst. Our study suggests that the water-gas shift reaction may not happen in Earth's upper mantle, and formic acid or formate may be an important carbon carrier in C-H-O fluids in a reduced environment, which participates in many geochemical processes in the deep carbon cycle, such as water-rock interactions and diamond formation in the mantle. Our findings highlight the diversity of aqueous carbon species in C-H-O fluids and the importance of organic geochemistry at extreme conditions.

We first dissolved 0.93 molal carbon monoxide (CO) into supercritical water at ∼10 and ∼13 GPa, 1400 K, the P-T conditions as found at the bottom of Earth's upper mantle. Figure 1 shows the mole percents of carbon-containing species as functions of simulation time in AIMD simulations. At ∼10 GPa, CO(aq) reacted with water to become formic acid

4

(HCOOH(aq)) after about 200 ps:

$$CO(aq) + H_2O \rightarrow HCOOH(aq). \qquad (2)$$
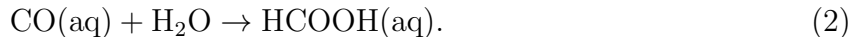
We continued the simulation up to 330 ps and found that HCOOH(aq) dissociated frequently; the main solutes were the HCOOH(aq) molecule and the formate ion (HCOO$^-$(aq)). When pressure was increased to $\sim$13 GPa, CO(aq) reacted with water faster, after only $\sim$30 ps. In the following $\sim$300 ps simulation, we found again that HCOOH(aq) and HCOO$^-$(aq) were the two major carbon species in the solution. At $\sim$13 GPa, it is also interesting to see formation of a minor carbon species, orthoformic acid (HC(OH)$_3$(aq) shown in Figure S1 in the supporting information), whose mole percent in total dissolved carbon was $\sim$2 %. The orthoformic acid molecules were formed by the reaction between HCOOH(aq) and water, and then rapidly dehydrated to become HCOOH(aq) via a reaction involving multiple water molecules within 2 ps.

To study the formation mechanism of aqueous formic acid (Figure 2), we carried out 6 AIMD simulations from uncorrelated initial configurations at $\sim$10 and $\sim$13 GPa, 1400 K (see Table SI in the supporting information). We found that the CO molecule and a few water molecules in solvation shells participated in the reaction. The carbon atom in the CO molecule formed a new C-O bond with an oxygen atom from a H$_2$O molecule or OH$^-$ ion. Within less than 100 fs this carbon atom also received a proton donated from a H$_3$O$^+$ ion or another H$_2$O molecule to form a C-H bond.

When the new C-O bond formed between the CO molecule and a H$_2$O molecule, the extra proton transferred to the solvent water molecules along hydrogen bond wires. When the new C-H bond formed between the CO molecule and a H$_2$O molecule, the remaining hydroxide ion either simply moved away or diffused by accepting a proton from neighboring water molecules. Overall, we found that the intense proton transfer and solvation interactions play a key role to generate HCOOH(aq). The reaction mechanism is fundamentally different from

that in the gas phase, where HCOOH(g) was considered as an intermediate in the water-gas shift reaction and only up to three water molecules participated.[35]

The almost simultaneously formed C-O and C-H bonds never broke after the formic acid molecule was generated, but HCOOH(aq) had very frequent acid dissociation reactions:

$$HCOOH(aq) \rightleftharpoons HCOO^-(aq) + H^+(aq). \tag{3}$$
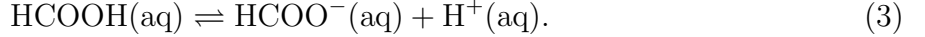
The dissociation constant, K_a, depends on P-T conditions as shown in Figure 3. With increasing pressure at 1000 K or 1400 K, K_a increases, while with increasing temperature along an isobar, K_a decreases. The trend of change is correlated with the variance of the dielectric constant of supercritical water, ϵ_0, as shown by previous first-principles and machine learning studies.[21,36] ϵ_0 increases with P and decreases with T, so the formate ion and proton are easier to separate with increasing P, but more difficult to separate with increasing T. At ambient conditions, formic acid is a weak acid with 1.3 % of HCOOH(aq) dissociating,[37] whereas at $\sim$13 GPa and 1400 K, our AIMD simulations showed that $\sim$62 % of HCOOH(aq) became ions. The predicted importance of the formate ion at elevated temperatures and pressures is consistent with recent aqueous speciation-solubility models of upper mantle fluids.[23]

The proton in reaction (3) kept hopping back and forth between formate and its surrounding water molecules in our simulations. Figure 4 shows the radial distribution functions (RDFs) of the carbon atom of formate versus the oxygen atoms of water (O_w) or hydronium ($O_{H_3O^+}$) at 10 and 13 GPa, and 1400 K. All RDFs have the main peaks at $\sim$3.1 Å, corresponding to the first solvation shells of formate. The first peak of the C-$O_{H_3O^+}$ RDF is taller than the first peak of the C-O_{H_2O} RDF at both $\sim$10 and $\sim$13 GPa, indicating that the H_3O^+(aq) ion tends to reside in the first solvation shell of HCOO$^-$(aq). With increasing pressure from $\sim$10 to $\sim$13 GPa, the first peak of the C-$O_{H_3O^+}$ RDF becomes lower, because the dielectric constant of water increases,[21,36] which weakens the ion pairing strength between HCOO$^-$(aq) and H_3O^+(aq).

6

In the industrial water-gas shift reaction, the products are CO_2 and H_2, and formic acid is considered as an intermediate in some reaction mechanisms. Our longest AIMD trajectory is about 340 ps, which is quite long as a first-principles simulation, but may be too short considering the reaction kinetics, so formic acid may decompose into CO_2 and H_2 later. To assess the thermodynamic stability of formic acid, we also studied the possible reaction between CO_2 and H_2 at extreme P-T conditions. In a simulation box, we mixed 20 CO_2 molecules and 20 H_2 molecules. At ∼13 GPa and 1400 K, we did not see any chemical reaction in a simulation nearly 300 ps long, whereas after increasing temperature to 2000 K and 2400 K at ∼14 GPa, we found the formation of formic acid again (see Figure S2):

$$CO_2 + H_2 \rightarrow HCOOH. \tag{4}$$

We continued the simulation at 2000 K for another ∼150 ps, and saw no further reaction of HCOOH. In CO_2 capture and storage, the hydrogenation of CO_2 to formic acid usually occurs in the presence of catalysts,[38] while our AIMD simulations show that the uncatalyzed reaction is possible at extreme P-T conditions.

The Gibbs free energy of reaction is $\Delta G = \Delta H - T\Delta S$, where ΔH is the enthalpy of reaction and ΔS is the entropy of reaction. Big molecules tend to break at high temperatures because a mixture of small molecules has a larger entropy and the entropy term $(-T\Delta S)$ in the Gibbs free energy dominates. However, when increasing temperature from 1400 K to 2000 K along an isobar, formic acid, a relatively larger molecule, can be spontaneously synthesized from CO_2 and H_2, indicating that reaction (4) is an enthalpically driven reaction. The enthalpy of reaction is $\Delta H = \Delta U + P\Delta V$, where ΔU is the internal energy of reaction and ΔV is the change of volume. The combination reaction (4) releases energy $(\Delta U < 0)$ and the volume also decreases at fixed pressure at supercritical states $(P\Delta V < 0)$, so ΔH is negative. Table SIV shows that the internal energies of both reactants and products increase with increasing P, whereas ΔU becomes more negative, as shown in Figure S3,

7

indicating that the repulsive interactions between formic acid molecules increase less than those between CO_2 and H_2 under higher pressure. The RDFs of the oxygen atoms of CO_2 versus the hydrogen atoms of H_2 show the first peak between 2.5 and 3 Å as shown in Figure S4(a), while the RDFs of the oxygen atoms of HCOOH versus the hydrogen atom in the hydroxyl group have the first peak between 1.5 and 2 Å, which is a typical length of hydrogen bonds. The first peak of $O-H_{OH}$ RDFs becomes taller when P increases in Figure S4(b), suggesting that the hydrogen bonding between formic acid molecules may help to soften the repulsive interactions.

At the lower temperature of 1400 K, the entropy term contributes less than at 2000 K, so the formation of formic acid should be even more favored. The reason we did not see formic acid in our AIMD simulation at 1400 K is that the reaction kinetics is slow and our simulation is not long enough.

To infer the possible P-T range for the formation of formic acid, We calculated the free energies of formic acid and the mixture of CO_2 and H_2 using the two-phase thermodynamic model[39–41] To validate our calculation method, we first compared the free energies of the reactants and products of the water-gas shift reaction at ∼10 MPa and 473 K. The enthalpy of reaction (ΔH) is -59.8 ± 1.8 kJ/mol, $T\Delta S$ is -1.0 ± 2.2 kJ/mol, and the free energy of reaction (ΔG) is -58.8 ± 2.8 kJ/mol, so the forward water-gas shift reaction is exothermic and thermodynamically favored, consistent with experimental findings. Spanu et al. applied the two-phase thermodynamic model to study the formation of heavier alkanes from methane, and found that the mixtures of longer alkanes and hydrogen are thermodynamically more stable than methane when P is above 4 GPa and T is between 1000 and 2000 K.[42] Our test and the previous study suggest that the two-phase thermodynamic model is capable to evaluate thermodynamic stability of C-H-O fluids at high P-T conditions.

We then increased pressure to ∼10 GPa and temperature to 1000 and 1400 K to calculate the free energy of reaction (4), as shown in Figure 5. We found that the mixture of CO_2 and H_2 is thermodynamically more favored than formic acid up to ∼0.8 GPa at 1000 K.

At higher pressures, reaction (4) may happen spontaneously. With increasing P along an isotherm, the reaction enthalpy becomes more negative, while the entropy term, $T\Delta S$, does not vary much, so formic acid becomes thermodynamically more stable than the mixture of CO_2 and H_2. When increasing temperature to 1400 K along an isobar, the free energy of reaction (4) becomes less negative, and formic acid is more favored when P > ~2.7 GPa. Our free energy calculations show that reaction (4) is exothermic and enthalpically driven.

Besides, our free energy calculations show that the mixture of CO_2 and H_2 is thermodynamically more stable than the mixture of CO and H_2O (see Figure S5). Hence, we found that formic acid is not a short-lived reaction intermediate in the water-gas shift reaction, but a thermodynamically favored product at P-T conditions typically found in Earth's upper mantle.

In our AIMD simulations, we mainly used the generalized gradient approximation exchange-correlation (xc) functional, PBE,[43] which has been found insufficient to describe aqueous systems at ambient conditions. We calculated the enthalpy of reaction (1) at ambient conditions, which is -63.3 kJ/mol at the PBE level of theory and -46.1 kJ/mol using PBE0, a hybrid xc functional with 25% Hartree-Fock exchange,[44] indicating that the PBE0 result is closer to the experimental value (-41 kJ/mol). However, our previous studies showed that the PBE functional works better at extreme P-T conditions than at ambient conditions.[21,27,45] For example, for CO_2 dissolved in supercritical water at ~11 GPa and 1000 K, PBE predicts similar carbon species concentrations to those obtained by PBE0. Spanu et al. applied the PBE functional to calculate the free energy difference of methane and a hydrogen and ethane mixture at zero pressure and 1000 K, which is 26.1 kJ per 1 mol carbon, comparable to the experimental value 34.7 kJ/mol.[42] Note that the long-range dispersion interactions are missing in both PBE and PBE0, but here the chemical reactions involve breaking and forming of covalent bonds, in which weak van der Waals interactions do not play a major role.

Formic acid and formate have been found in natural waters in some shallow crustal

9

environments, such as spring waters, fluids in sedimentary basin and hydrothermal fluids, where pressure is lower than 50 MPa and temperature is up to about 673 K.[46,47] At high P-T or in the presence of catalysts, formic acid may decompose through the decarboxylation reaction:[48]

$$HCOOH \rightarrow CO_2 + H_2, \tag{5}$$

or the dehydration reaction:

$$HCOOH \rightarrow CO + H_2O. \tag{6}$$

Previous studies found that the decarboxylation reaction predominates in aqueous environments, while dehydration happens more in gas phases.[47,48] Thus, formic acid or formate has often been viewed as a reaction intermediate in the abiotic reduction of oxidized carbon to hydrocarbons or in the decomposition of bigger organic molecules. In the laboratory, as it is more convenient to load liquids to a reaction cell, some experiments started from HCOOH(l) to generate a mixture of CO_2, H_2, CO and H_2O through reaction (5) and (6).[18,49]

With increasing P and T in Earth's upper mantle, traditional geochemical models for C-H-O fluids focused on simple mixtures of small volatile molecules, such as H_2O, CO_2, CO, C_2H_6, H_2, O_2,[19] whereas recent first-principles simulations, geochemical models, and high P-T experiments suggest that fully oxidized carbon may largely exist as HCO_3^- and CO_3^{2-} ions, and H_2CO_3(aq) in water, not only non-interactive CO_2(aq) molecules.[26–29] In Earth's mantle, the oxygen fugacity, f_{O_2}, reflects the mantle oxidation state, which greatly influences the speciation of C-H-O fluids. With increasing depth, f_{O_2} generally decreases, so the upper mantle likely becomes more reducing at the bottom.[30] Contrary to the commonly accepted assumption that the water-gas shift reaction may adjust the composition of C-H-O fluids in a reducing environment,[18,31] we found CO may react with H_2O to generate formic acid, which is a thermodynamically stable product. Thus, formic acid or formate may be an important reduced carbon carrier in C-H-O fluids in Earth's upper mantle, and participates in many geochemical processes.

In our simulations, formic acid can easily dissociate in water at extreme P-T conditions as shown in Figure 3. For example, in a 0.94 molal solution of HCOOH(aq) at ∼13 GPa and 1400 K, the concentration of H_3O^+(aq) is ∼0.58 molal larger than that of OH^-(aq), so the presence of HCOOH(aq) greatly affects the acidity of aqueous solutions in a reducing environment and may influence water-rock interactions in deep Earth.[50] It was recently reported that infiltrating C-H-O fluids may dissolve a great amount of carbonate minerals in subducting slabs, and bring carbon back to magmas, which may be finally released as CO_2 from volcanoes;[51,52] however, we have not yet known the chemical mechanism of this dissolution. It is possible that reduced carbon forms formic acid, which helps to dissolve carbonate minerals into C-H-O fluids in the deep carbon cycle. The dissociation of formic acid could also promote the formation of metal-formate, i.e. organometallic, complexes in upper mantle fluids.[23]

Formic acid or formate may also participate into the formation of diamonds in Earth's upper mantle, as indicated by the newly developed Deep Earth Water (DEW) model[6,8] and experiments.[7] Sverjensky and Huang found that the diamond formation may be associated with a pH drop, and most of precipitated diamonds come from the destruction of formate:[6]

$$HCOO^-(aq) + H^+(aq) + H_2(aq) \rightarrow C(diamond) + 2H_2O, \tag{7}$$

In the formation of diamonds from the Panda kimberlite, formate contributes to 2.2 out of 13.8 mol of carbon in diamonds:[8]

$$3HCOO^-(aq) + 3H^+(aq) + C_2H_6(aq) \rightarrow 5C(diamond) + 6H_2O. \tag{8}$$
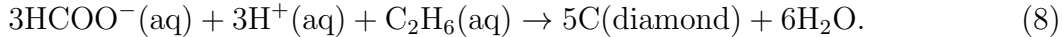
Using Raman spectroscopy measurements, Frezzotti found the surfaces of diamonds in metamorphic rocks from Lago di Cignana in Italy are coated by functional groups of carboxylic acids, indicating that organic acids play an important role in nucleation and growth of diamonds in deep Earth.[7]

In summary, we performed extensive AIMD simulations and free energy calculations to study the water-gas shift reaction at extreme P-T conditions found in Earth's upper mantle. We found that CO directly reacts with H_2O to generate formic acid at 10~13 GPa and 1400 K without any catalyst. HCOOH(aq) dissociates frequently in supercritical water and greatly affects the pH of the solutions. It is commonly assumed that HCOOH or $HCOO^-$ is an intermediate product and will finally decompose in the water-gas shift reaction; however, our free energy calculations based on the AIMD simulation trajectories show that HCOOH is thermodynamically more favored than the mixture of CO_2 and H_2 above 3 GPa and at 1000~1400 K.

Our study suggests that formic acid or formate may be an important reduced carbon carrier in the deep carbon cycle. The presence of HCOOH(aq) increases the acidity of aqueous geofluids, and helps to dissolve carbonate minerals. C-H-O fluids may carry $HCOO^-$, CO_3^{2-}, HCO_3^-, H_2CO_3(aq), CO_2(aq) etc. into magmas, which may decompose near Earth's surface and be finally released as CO_2 from volcanoes. Formate may also be a key reactant in the formation of diamonds in the mantle. The stability of formic acid at P-T conditions in Earth's upper mantle suggests that Fischer-Tropsch-type synthesis in deep Earth may differ dramatically from hydrocarbon synthesis at industrial P-T conditions or in shallow Earth environments. Our findings highlight the diversity of aqueous carbon species in C-H-O geofluids and the importance of organic geochemistry at extreme conditions.

Methods

We performed AIMD simulations within the Born-Oppenheimer approximation using the Qbox code (http://qboxcode.org/).[53] We used the PBE exchange-correlation functional[43] and plane-wave basis sets with periodic boundary conditions. We used norm-conserving pseudopotentials[54,55] and employed a kinetic energy cutoff of 85 Ry, which was increased to 145 Ry to compute pressure. The Brillouin zone was sampled at the Γ-point only. We

used deuterium instead of hydrogen in the simulations, allowing for a larger time step (0.24 fs). We still refer to these atoms as hydrogen atoms in the main text for convenience. The temperature was controlled by stochastic rescaling of the velocities with a damping factor of 24.2 fs.[56] After an equilibration of at least 5 ps at each P-T condition, we ran AIMD simulations of ~300 ps long to detect chemical reactions (see Table SI in the supporting information).

To determine the carbon species in our AIMD simulations of CO(aq), we analyzed the atomic trajectories in each frame and searched for the three nearest O atoms to the C atom, whose distances are d_{C-O1}, d_{C-O2}, and d_{C-O3} from small to large. If d_{C-O2} is larger than d_{C-O1} by more than 0.4 Å, the molecule is considered as CO; otherwise the C atom is bonded with at least two O atoms, and additionally if $d_{C-O3} - d_{C-O2} < 0.4$ Å, the C atom is bonded with three O atoms. H atoms were considered bonded to their nearest-neighbor C or O atom. Using this method, we may distinguish CO, HCOOH, HCOO$^-$, HCOOH$_2^+$, HC(OH)$_3$, and orthoformic acid derivatives.

We used the two-phase thermodynamic model introduced in refs 39–41 to calculate the free energies of reactants and products. In this method, entropy is divided into translational, rotational, and vibrational parts, which were obtained from corresponding phonon densities of states (DOS). The translational and rotational phonon DOS contain solid-like and gas-like parts. The phonon DOS were calculated by the Fourier transform of velocity auto-correlation functions from AIMD trajectories, each of which is at least 20 ps long (Table SIII in the supporting information). In case proton transfer occurs, the contribution of the ith chemical species to the total entropy is weighted by $\frac{\tau_i}{t_{tot}}$, where τ_i is its life time and t_{tot} is the total simulation time.[57]

Acknowledgements

Supporting Information Available:

AIMD simulation setups, computational cost, reaction products of CO(aq), the orthoformic acid molecule, reaction mechanism of $CO_2 + H_2 \rightarrow HCOOH$, thermodynamic quantities of C-H-O fluids obtained from AIMD simulations, O-H RDFs for $CO_2 + H_2$ and HCOOH simulations, free energy of the water-gas shift reaction at 1000 K.

References

(1) Falkowski, P.; Scholes, R. J.; Boyle, E.; Canadell, J.; Canfield, D.; Elser, J.; Gruber, N.; Hibbard, K.; Högberg, P.; Linder, S. et al. The Global Carbon Cycle: A Test of Our Knowledge of Earth as a System. *Science* **2000**, *290*, 291–296.

(2) Hazen, R. M.; Schiffries, C. M. Why Deep Carbon? *Rev. Mineral. Geochem.* **2013**, *75*, 1–6.

(3) Mendeleev, D. L'Origine du Pétrole. *Rev. Sci.* **1877**, *8*, 409–416.

(4) McCollom, T. M. Laboratory Simulations of Abiotic Hydrocarbon Formation in Earth's Deep Subsurface. *Rev. Mineral. Geochem.* **2013**, *75*, 467–494.

14

(5) Sephton, M. A.; Hazen, R. M. On the Origins of Deep Hydrocarbons. *Rev. Mineral. Geochem.* **2013**, *75*, 449–465.

(6) Sverjensky, D. A.; Huang, F. Diamond Formation Due to a pH Drop During Fluid-Rock Interactions. *Nat. Commun.* **2015**, *6*, 8702.

(7) Frezzotti, M. L. Diamond Growth From Organic Compounds in Hydrous Fluids Deep Within the Earth. *Nat. Commun.* **2019**, *10*, 4952.

(8) Huang, F.; Sverjensky, D. A. Mixing of Carbonatitic into Saline Fluid During Panda Diamond Formation. *Geochim. Cosmochim. Acta* **2020**, *284*, 1–20.

(9) Sobolev, N. V.; Logvinova, A. M.; Tomilenko, A. A.; Wirth, R.; Bul'bak, T. A.; Luk'yanova, L. I.; Fedorova, E. N.; Reutsky, V. N.; Efimova, E. S. Mineral and Fluid Inclusions in Diamonds from the Urals Placers, Russia: Evidence for Solid Molecular N_2 and Hydrocarbons in Fluid Inclusions. *Geochim. Cosmochim. Acta* **2019**, *266*, 197–219.

(10) Daniel, I.; Oger, P.; Winter, R. Origins of Life and Biochemistry under High-Pressure Conditions. *Chem. Soc. Rev.* **2006**, *35*, 858–875.

(11) Frost, D. J. The Upper Mantle and Transition Zone. *Elements* **2008**, *4*, 171–176.

(12) Lobanov, S. S.; Chen, P.-N.; Chen, X.-J.; Zha, C.-S.; Litasov, K. D.; Mao, H.-K.; Goncharov, A. F. Carbon Precipitation from Heavy Hydrocarbon Fluid in Deep Planetary Interiors. *Nat. Commun.* **2013**, *4*, 2446.

(13) Dry, M. E. The Fischer–Tropsch Process: 1950–2000. *Catal. Today* **2002**, *71*, 227–241.

(14) Bukur, D. B.; Todic, B.; Elbashir, N. Role of Water-Gas-Shift Reaction in Fischer-Tropsch Synthesis on Iron Catalysts: A Review. *Catal. Today* **2016**, *275*, 66–75.

(15) Ratnasamy, C.; Wagner, J. P. Water Gas Shift Catalysis. *Catal. Rev.* **2009**, *51*, 325–440.

(16) Shido, T.; Iwasawa, Y. Reactant-Promoted Reaction Mechanism for Water-Gas Shift Reaction on Rh-doped CeO_2. *J. Catal.* **1993**, *141*, 71–81.

(17) Yoshida, K.; Wakai, C.; Matubayasi, N.; Nakahara, M. NMR Spectroscopic Evidence for an Intermediate of Formic Acid in the Water-Gas-Shift Reaction. *J. Phys. Chem. A* **2004**, *108*, 7479–7482.

(18) Sharma, A.; Cody, G. D.; Hemley, R. J. In Situ Diamond-Anvil Cell Observations of Methanogenesis at High Pressures and Temperatures. *Energy Fuels* **2009**, *23*, 5571–5579.

(19) Zhang, C.; Duan, Z. A Model for C-O-H Fluid in the Earth's Mantle. *Geochim. Cosmochim. Acta* **2009**, *73*, 2089–2102.

(20) Manning, C. E.; Shock, E. L.; Sverjensky, D. A. The Chemistry of Carbon in Aqueous Fluids at Crustal and Upper Mantle Conditions: Experimental and Theoretical Constraints. *Rev. Mineral. Geochem.* **2013**, *75*, 109–148.

(21) Pan, D.; Spanu, L.; Harrison, B.; Sverjensky, D. A.; Galli, G. Dielectric Properties of Water under Extreme Conditions and Transport of Carbonates in the Deep Earth. *Proc. Natl. Acad. Sci. U. S. A.* **2013**, *110*, 6646–6650.

(22) Sverjensky, D. A.; Stagno, V.; Huang, F. Important Role for Organic Carbon in Subduction-Zone Fluids in the Deep Carbon Cycle. *Nat. Geosci.* **2014**, *7*, 909–913.

(23) Huang, F.; Sverjensky, D. A. Extended Deep Earth Water Model for Predicting Major Element Mantle Metasomatism. *Geochim. Cosmochim. Acta* **2019**, *254*, 192–230.

(24) Sverjensky, D. A. Thermodynamic Modelling of Fluids from Surficial to Mantle Conditions. *J. Geol. Soc.* **2019**, *176*, 348–374.

(25) Sverjensky, D. A.; Daniel, I.; Brovarone, A. V. In *Carbon in Earth's Interior*; Manning, C. E., Lin, J.-F., Mao, W. L., Eds.; John Wiley & Sons, Inc.: Hoboken, NJ, 2020; Chapter 22, pp 259–269.

(26) Facq, S.; Daniel, I.; Montagnac, G.; Cardon, H.; Sverjensky, D. A. In Situ Raman Study and Thermodynamic Model of Aqueous Carbonate Speciation in Equilibrium with Aragonite under Subduction Zone Conditions. *Geochim. Cosmochim. Acta* **2014**, *132*, 375–390.

(27) Pan, D.; Galli, G. The Fate of Carbon Dioxide in Water-Rich Fluids under Extreme Conditions. *Sci. Adv.* **2016**, *2*, e1601278.

(28) Abramson, E. H.; Bollengier, O.; Brown, J. M. The Water-Carbon Dioxide Miscibility Surface to 450 °C and 7 GPa. *Am. J. Sci.* **2017**, *317*, 967–989.

(29) Stolte, N.; Pan, D. Large Presence of Carbonic Acid in CO_2-Rich Aqueous Fluids under Earth's Mantle Conditions. *J. Phys. Chem. Lett.* **2019**, *10*, 5135–5141.

(30) Frost, D. J.; McCammon, C. A. The Redox State of Earth's Mantle. *Annu. Rev. Earth Planet. Sci.* **2008**, *36*, 389–420.

(31) McCollom, T. M.; Seewald, J. S. Carbon Isotope Composition of Organic Compounds Produced by Abiotic Synthesis under Hydrothermal Conditions. *Earth Planet. Sci. Lett.* **2006**, *243*, 74–84.

(32) Cavazzoni, C.; Chiarotti, G. L.; Scandolo, S.; Tosatti, E.; Bernasconi, M.; Parrinello, M. Superionic and Metallic States of Water and Ammonia at Giant Planet Conditions. *Science* **1999**, *283*, 44–46.

(33) Gygi, F.; Galli, G. Ab Initio Simulation in Extreme Conditions. *Mater. Today* **2005**, *8*, 26–32.

(34) Sun, J.; Klug, D. D.; Martoňák, R.; Montoya, J. A.; Lee, M.-S.; Scandolo, S.; Tosatti, E. High-pressure Polymeric Phases of Carbon Dioxide. *Proc. Natl. Acad. Sci. U. S. A.* **2009**, *106*, 6077–6081.

(35) Melius, C. F.; Bergan, N. E.; Shepherd, J. E. Effects of Water on Combustion Kinetics at High Pressure. *Symp. (Int.) Combust.* **1991**, *23*, 217–223.

(36) Hou, R.; Quan, Y.; Pan, D. Dielectric Constant of Supercritical Water in a Large Pressure–Temperature Range. *J. Chem. Phys.* **2020**, *153*, 101103.

(37) Tro, N. K. *Chemistry: A Molecular Approach*; Pearson Education, Inc.: Hoboken, NJ, 2020.

(38) Álvarez, A.; Bansode, A.; Urakawa, A.; Bavykina, A. V.; Wezendonk, T. A.; Makkee, M.; Gascon, J.; Kapteijn, F. Challenges in the Greener Production of Formates/Formic Acid, Methanol, and DME by Heterogeneously Catalyzed CO_2 Hydrogenation Processes. *Chem. Rev.* **2017**, *117*, 9804–9838.

(39) Lin, S.-T.; Blanco, M.; Goddard, W. A. The Two-Phase Model for Calculating Thermodynamic Properties of Liquids from Molecular Dynamics: Validation for the Phase Diagram of Lennard-Jones Fluids. *J. Chem. Phys.* **2003**, *119*, 11792–11805.

(40) Lin, S.-T.; Maiti, P. K.; Goddard III, W. A. Two-Phase Thermodynamic Model for Efficient and Accurate Absolute Entropy of Water from Molecular Dynamics Simulations. *J. Phys. Chem. B* **2010**, *114*, 8191–8198.

(41) Lai, P.-K.; Hsieh, C.-M.; Lin, S.-T. Rapid Determination of Entropy and Free Energy of Mixtures from Molecular Dynamics Simulations with the Two-Phase Thermodynamic Model. *Phys. Chem. Chem. Phys.* **2012**, *14*, 15206–15213.

(42) Spanu, L.; Donadio, D.; Hohl, D.; Schwegler, E.; Galli, G. Stability of Hydrocarbons at

Deep Earth Pressures and Temperatures. *Proc. Natl. Acad. Sci. U. S. A.* **2011**, *108*, 6843–6846.

(43) Perdew, J. P.; Burke, K.; Ernzerhof, M. Generalized Gradient Approximation Made Simple. *Phys. Rev. Lett.* **1996**, *77*, 3865–3868.

(44) Adamo, C.; Barone, V. Toward Reliable Density Functional Methods without Adjustable Parameters: The PBE0 Model. *J. Chem. Phys.* **1999**, *110*, 6158–6170.

(45) Pan, D.; Wan, Q.; Galli, G. The Refractive Index and Electronic Gap of Water and Ice Increase with Increasing Pressure. *Nat. Commun.* **2014**, *5*, 3919.

(46) Zeng, Y.; Liu, J. Short-Chain Carboxylates in Fluid Inclusions in Minerals. *Appl. Geochem.* **2000**, *15*, 13–25.

(47) McCollom, T. M.; Seewald, J. S. Experimental Constraints on the Hydrothermal Reactivity of Organic Acids and Acid Anions: I. Formic Acid and Formate. *Geochim. Cosmochim. Acta* **2003**, *67*, 3625–3644.

(48) Yu, J.; Savage, P. E. Decomposition of Formic Acid under Hydrothermal Conditions. *Ind. Eng. Chem. Res.* **1998**, *37*, 2–10.

(49) Seewald, J. S.; Zolotov, M. Y.; McCollom, T. M. Experimental Investigation of Single Carbon Compounds under Hydrothermal Conditions. *Geochim. Cosmochim. Acta* **2006**, *70*, 446–460.

(50) Galvez, M. E.; Connolly, J. A. D.; Manning, C. E. Implications for Metal and Volatile Cycles from the pH of Subduction Zone Fluids. *Nature* **2016**, *539*, 420–424.

(51) Ague, J. J.; Nicolescu, S. Carbon Dioxide Released from Subduction Zones by Fluid-Mediated Reactions. *Nat. Geosci.* **2014**, *7*, 355–360.

(52) Manning, C. E. A Piece of the Deep Carbon Puzzle. *Nature Geosci.* **2014**, *7*, 333–334.

(53) Gygi, F. Architecture of Qbox: A Scalable First-Principles Molecular Dynamics Code. *IBM J. Res. Dev.* **2008**, *52*, 137–144.

(54) Hamann, D. R.; Schlüter, M.; Chiang, C. Norm-Conserving Pseudopotentials. *Phys. Rev. Lett.* **1979**, *43*, 1494–1497.

(55) Vanderbilt, D. Optimally Smooth Norm-Conserving Pseudopotentials. *Phys. Rev. B* **1985**, *32*, 8412–8415.

(56) Bussi, G.; Donadio, D.; Parrinello, M. Canonical Sampling Through Velocity Rescaling. *J. Chem. Phys.* **2007**, *126*, 014101.

(57) Caro, M. A.; Lopez-Acevedo, O.; Laurila, T. Redox Potentials from Ab Initio Molecular Dynamics and Explicit Entropy Calculations: Application to Transition Metals in Aqueous Solution. *J. Chem. Theory Comput.* **2017**, *13*, 3432–3441.

(58) Flyvbjerg, H.; Petersen, H. G. Error Estimates on Averages of Correlated Data. *J. Chem. Phys.* **1989**, *91*, 461–466.
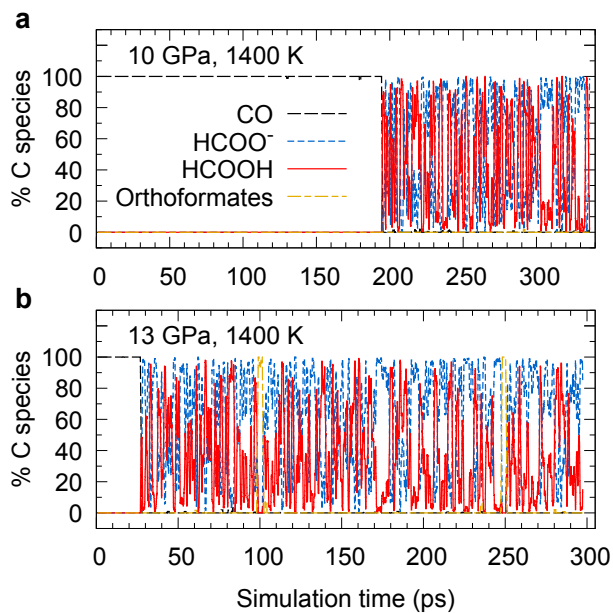
Figure 1: Mole percents of CO(aq), HCOO$^-$(aq), HCOOH(aq), and orthoformates as functions of simulation time in AIMD simulations. Initially, 0.93 molal CO(aq) was dissolved in supercritical water. Two P-T conditions, (a) 10 GPa, 1400 K and (b) 13 GPa, 1400 K, were compared. Orthoformates include orthoformic acid (HC(OH)$_3$(aq)) and its conjugate bases (CH$_3$O$_3^-$(aq), CH$_2$O$_3^{2-}$(aq), CHO$_3^{3-}$(aq)). The mole percents were calculated by 1-ps moving average.
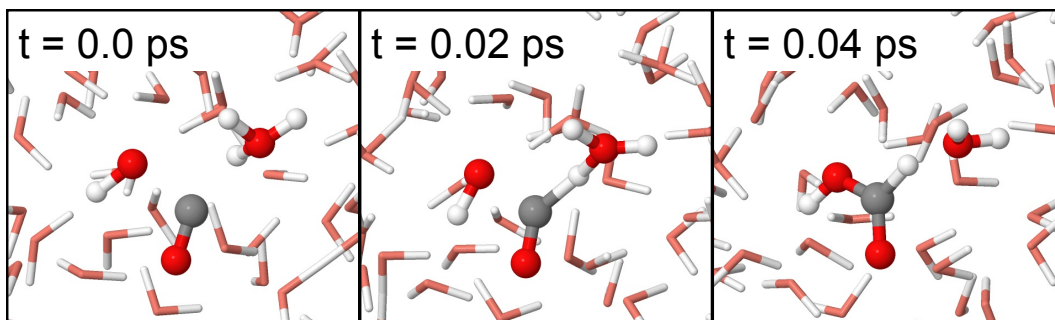
Figure 2: Formation of formic acid from CO(aq) at ~10 GPa, 1400 K. The carbon atom formed a new C-O bond with the oxygen atom from a OH^- ion, and almost simultaneously a H_3O^+ ion donated a proton to the carbon atom.
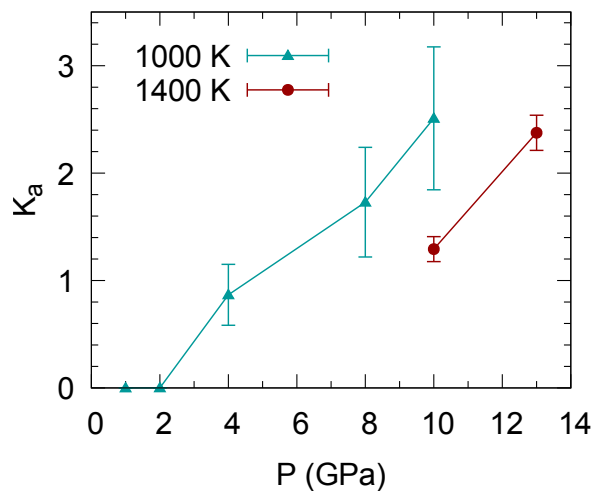

Figure 3: Acid dissociation constant of HCOOH(aq), $K_a = \frac{[\text{HCOO}^-][\text{H}^+]}{[\text{HCOOH}]}$, as a function of pressure at 1000 and 1400 K. Error bars were obtained using the blocking method.[58] The lines connecting points are a guide to the eye.
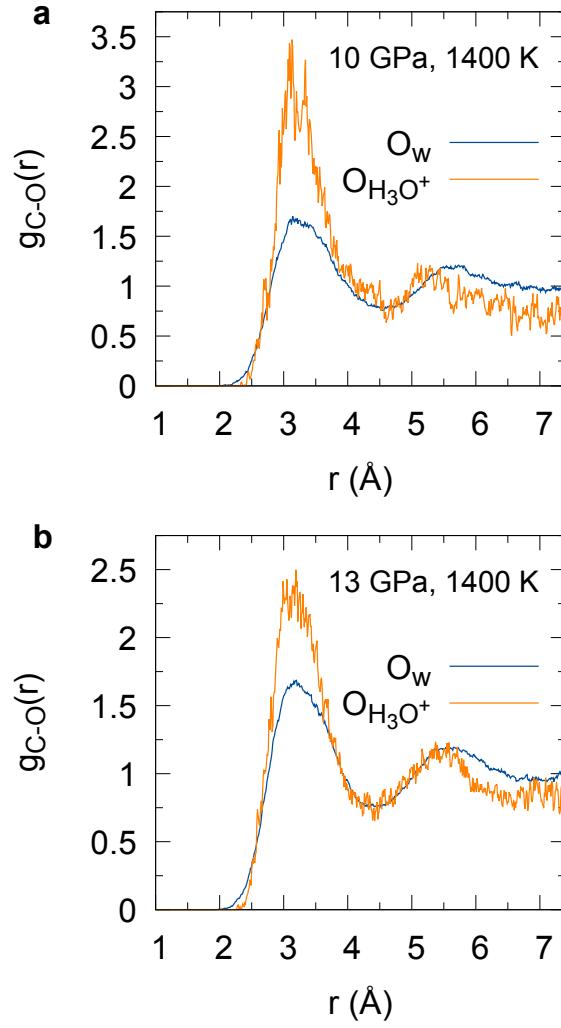
Figure 4: Radial distribution functions of the carbon atom of formate versus the oxygen atoms of H_2O (O_w) or H_3O^+(aq) ($O_{H_3O^+}$). The molality of $HCOO^-$(aq) is 0.94 molal. Two P-T conditions, (a) $\sim$10 GPa, 1400 K and (b) $\sim$13 GPa, 1400 K, were compared.
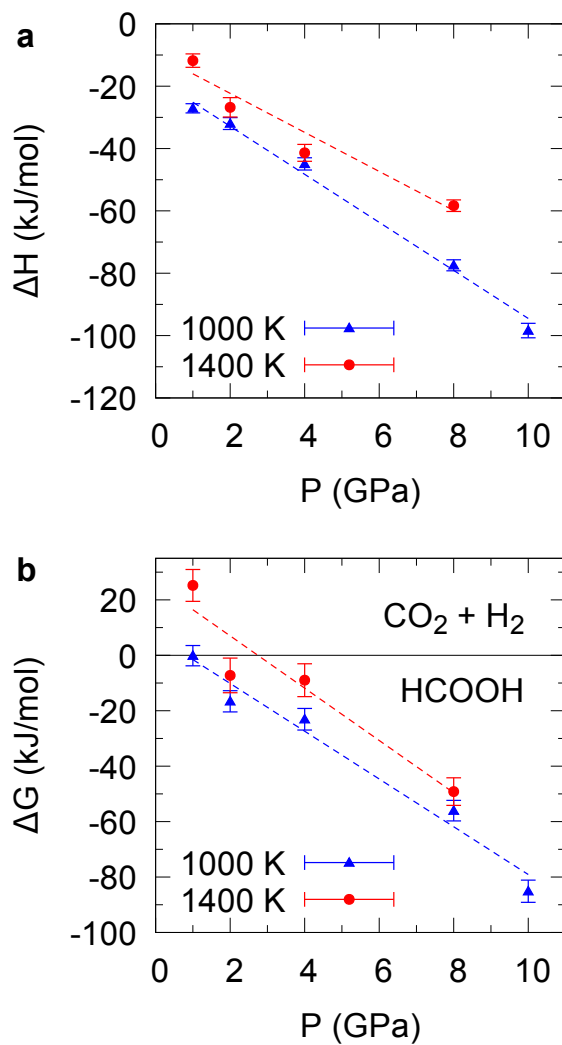
Figure 5: Reaction enthalpies (a) and free energies (b) of the formation of HCOOH from CO_2 and H_2 as functions of pressure. Two temperatures were compared: 1000 and 1400 K. Error bars were obtained using the blocking method.[58] Dashed lines show the linear fit of first-principles data.